



Petrology, Geochemistry (Isotopic Geochemistry)

Evidence of heterogeneous crustal origin for the Pan-African Mbengwi granitoids and the associated mafic intrusions (northwestern Cameroon, central Africa)



Benoît Joseph Mbassa^{a,*}, Pierre Kamgang^b, Michel Grégoire^c, Emmanuel Njonfang^d, Mathieu Benoit^c, Zénon Itiga^a, Stéphanie Duchene^c, Moïse Bessong^e, Pauline Wonkwenmendam Nguet^a, Ntepe Nfomou^a

^a Institut de recherches géologiques et minières, Antenne de recherches géophysiques et volcanologiques Ekona, BP 370, Buea, Cameroon

^b Département des sciences de la Terre et de l'Univers, Faculté des sciences, Université de Yaoundé-I, BP 812, Yaoundé, Cameroon

^c Géosciences-Environnement-Toulouse, UMR 5563, Observatoire Midi Pyrénées, Université Paul-Sabatier, 14, avenue Édouard-Belin, 31400 Toulouse, France

^d Laboratoire de géologie, École normale supérieure, Université de Yaoundé-I, BP 47, Yaoundé, Cameroon

^e Institut de recherches géologiques et minières, Laboratoire de traitement des minéraux, BP 4110, Yaoundé, Cameroon

ARTICLE INFO

Article history:

Received 28 August 2015

Accepted after revision 22 September 2015

Available online 5 February 2016

Handled by Isabelle Manighetti

Keywords:

High-K calc-alkaline plutonics

Metaluminous to weakly peraluminous

Type I

Lower continental crust

Subduction signature

Cameroon

ABSTRACT

The Mbengwi plutonics consist of intermediate to felsic granitoids forming a continuous magmatic series from monzonite to granite and mafic intrusions. Their mineralogical composition consists of quartz, plagioclases, K-feldspars, biotite, muscovite, and amphibole. The accessory phase includes opaque minerals + titanite ± apatite ± zircon, while secondary minerals are pyrite, phengite, chlorite, epidote, and rarely calcite. These plutonics are assigned high-K calc-alkaline to shoshonitic series, metaluminous to weakly peraluminous and mostly belong to an I-type suite ($A/CNK = 0.63–1.2$). They are typically post-collisional, with a subduction signature probably being inherited from their protoliths emplaced during the subduction phase. The Sr and Nd isotopic data evidence that these plutonics result from melting of the lower continental crust with variable contribution of the oceanic crust. Their geochemical features are similar to those of western Cameroon granitoids related to the Pan-African D₁ event in Cameroon.

© 2015 Académie des sciences. Published by Elsevier Masson SAS. All rights reserved.

1. Introduction

The Pan-African orogen in Cameroon is represented by the Central African fold belt (CAFB) (Toteu et al., 2004), which extends from Cameroon to Sudan (Fig. 1), and which resulted from the collision between the former São Francisco-Congo craton, the West African craton and the East Sahara metacraton (Ngako et al.,

2008). It includes meta-volcano-sedimentary series and granitoids (Fig. 1b). The granitoids cover a significant surface both in central and western Cameroon, including the Mbengwi massif, not yet been investigated in detail and derived from anatexic melting of the continental crust or from a juvenile lithospheric mantle (Djouka-Fonkwe et al., 2008; Kwékam et al., 2010; Mbassa, 2015). The present paper provides detailed petrographic features, major elements and Sr and Nd isotopic data of the Mbengwi plutonics in order to better constrain their magmatic sources and their contribution to the evolution of the CAFB in Cameroon.

* Corresponding author.

E-mail address: benjo_mbassa@yahoo.fr (B.J. Mbassa).

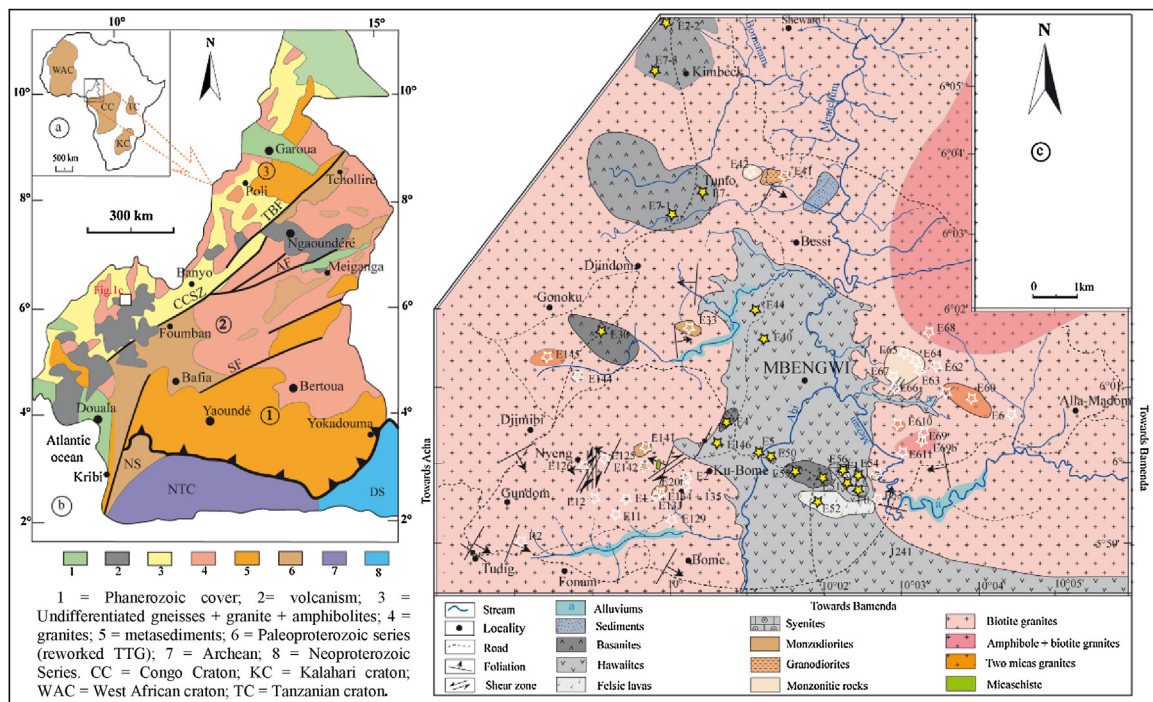


Fig. 1. Geological setting of the studied area; (a) location of Cameroon in Africa; (b) simplified geological map of Cameroon showing the main Pan–African domains. AF: Adamawa fault; SF: Sanaga fault; TBF: Tcholliré–Banyo fault; CCSZ: central Cameroon shear zone; NTC: Ntem complex; DS: Dja series; NS: Nyong series. **1:** southern; **2:** central domain; **3:** northern domain; (c) Geologic sketch map of the studied area. The white stars represent the studied plutonic rocks; the filled stars are for the alkaline series studied by Mbassa et al. (2012).

2. Geological background

The Pan–African fold belt in Cameroon is divided into three domains (Toteu et al., 2004):

- the southern domain that comprises Pan–African meta-sedimentary units (Nzenti et al., 1988; Ngnotué et al., 2000) and was thrusted onto the Archean Congo craton towards the south (Nédélec et al., 1986);
- the central domain, located between the Sanaga fault and the Tcholliré–Banyo fault, comprises the Adamawa fault and other anastomosed faults, which constitute the Central Cameroon shear zone (CCSZ) system (Fig. 1b);
- the northern domain, which contains the study area and has been affected by at least two magmatic episodes related to the Pan–African orogeny. The older one (640–620 Ma) corresponds to pre- to syn-tectonic calc-alkaline granitoids emplacement and the younger one (\approx 580 Ma) to late tectonic granitoids emplacement (Penaye et al., 1989; Toteu et al., 2001).

The tectonic evolution of the Pan–African belt in central and southern Cameroon is characterized by transpressive movements. The resulting structures include the N70E sinistral shear zones of central Cameroon (CCSZ and SF) and the granulitic and migmatitic thrust sheets overriding the Congo craton (Njanko et al., 2006).

Structurally, four Pan–African regional deformation tectonic phases have been recognized in Cameroon (Toteu et al., 2004) and have been recently identified by Ngako

et al. (2008) as corresponding to three successive tectonic events:

- crustal thickening (630–620 Ma);
- left lateral wrench movements (613–585 Ma);
- right lateral wrench movements (585–540 Ma), mainly marked by the CCSZ.

The studied area, geographically bounded by the latitudes $6^{\circ}06'$ and $5^{\circ}58'$ north and the longitudes $9^{\circ}57'$ and $10^{\circ}06'$ east (Fig. 1c), is marked by the abundance of Pan–African basement rocks relative to Tertiary magmatic and sedimentary rocks.

3. Petrography

Plutonic rocks from Mbengwi consist of coarse-grained felsic granitoids and fine-grained mafic rocks. Granitoids comprise monzonite, Qtz-monzonite, granodiorite and granites, showing a mylonitic structure (Fig. 2a and b). The fine-grained mafic rocks are monzodiorites and outcrop as small subrounded or elongated enclaves within granitoids. The main mineral phase assemblage of the studied rocks made up of K-feldspar (Kfs), plagioclase (Pl), quartz (Qtz), amphibole and biotite (Bt) is completed by muscovite (Ms) in two-mica granite. The accessory phase consists of opaque minerals, sphene (Spn), apatite (Ap), zircon (Zrn). Due to later alteration processes, Bt is locally replaced with chlorite (Chl) or prehnite (Prh), amphiboles with Chl, epidote (Ep) or calcite, iron–oxides with goethite,

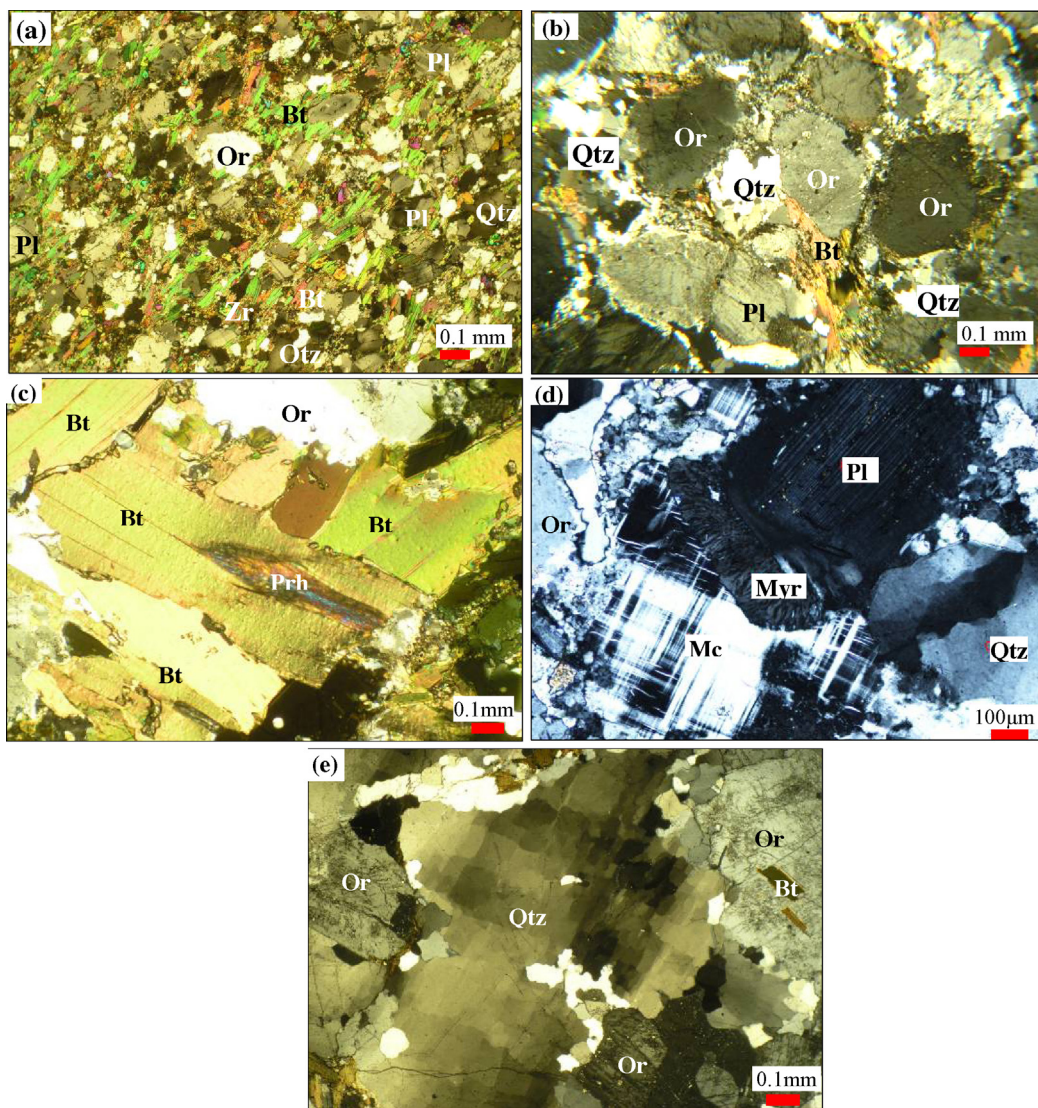


Fig. 2. Photomicrographs of thin sections of some plutonics from Mbengwi. Mineral symbols are after Kretz (1983). (a) Grano-lepidoblastic texture in a Bt-granite (E_{124}); (b) granoblastic texture in an amphibole-Bt-granite; (c): alteration of a biotite to prehnite; (d) spark perthites and myrmekites in a microcline crystal; (e): recrystallized Qtz phenocrysts.

while sericite needles crystallized at the expense of feldspars.

Monzodiorites (mafic enclaves) are dark grey. Qtz ($\leq 2\%$) is interstitial or clogs the cracks affecting feldspars or amphiboles. Plagioclase (15–30%) is oligoclase or andesine (An_{27-42}), often enclosing amphiboles, Bt, Spn and opaque minerals or included in Kfs. Kfs (5–8%) are perthitic orthoclase crystals (Or_{90-92}), enclosing Bt, pyrite and Spn. Amphibole (30–47%) has a composition of actinolite, edenite, Mg-hornblende or Mg-hastingsite. Phenocrysts are often zoned and poikilitic (Bt + Spn + Ap + opaque minerals). Mg-biotite (15–28%) are fine flakes, often altered into prehnite (Fig. 2c). Sphene mostly crystallizes around opaque minerals.

In monzonites, Qtz (10–15%) is concentrated in the microcrystalline phase. Plagioclase (25–30%) (An_{15-50}) is

often zoned and encloses amphibole, Mag or Spn. Orthoclase (20–25%; $Ab_{7-9}Or_{90-93}$) is perthitic and locally transformed into Mc. Amphiboles (15–20%) are brown to green pleochroic crystals of edenite, Fe-edenite or Fe-hornblende, which often constitute polycrystalline agglomerates associated with Mg-biotite, Spn, and Mag.

In Qtz-monzonites, Qtz (15–20%) is interstitial and occurs as rounded microcrystals or recrystallized microphenocrystals. Plagioclases phenocrysts (An_{9-46}) enclose Bt, Spn, Zrn, (Mag), Ap and Chl, while microcrystals are locally included in Mc. Orthoclase and microcline (25–30%) porphyrocrystals are poikilitic (Mag + Bt + Zrn + Spn + Pl + Ap) with frequent spark perthites and myrmekites (Fig. 2d). Brown or greenish Fe- or Mg- biotite (8–15%) enclose Ap or Mag. Amphiboles (4–7%) are composed of Fe-Hbl, hastingsite, Fe-edenite and often enclose feldspars

or Bt. Sphene (1–3%) has a lozenge shape. Zircon exhibits a polygonal or cubic shape, and is included in Mag, Spn or Bt. Apatite is interstitial or included in Spn.

In *granodiorites*, Qtz (20–25%) clogs cracks affecting feldspars. Plagioclase (30–35%) is oligoclase ($An_{18–28}$) often enclosing Bt, Chl or opaque minerals, or included in microcline (Mc). Orthoclase or Mc (12–15%) are xenomorphic or tabular. Amphibole (8–10%) is a Fe-hornblende. Phenocrysts enclose Spn, and microcrystals are interstitial. Biotite (8–10%) is interstitial or included in feldspars. Magnetite (< 1%) phenocrysts frequently show Spn recrystallization at their rim. Zircon occurs as bluish microcrystals with hexagonal shape, generally in inclusion. Apatite is often associated with Kfs. Chlorite flakes are bluish and show Bt core or Spn inclusions.

In *Bt-granites*, Qtz (30–40%) occurs in recrystallized grains exhibiting undulating extinction. Plagioclases (10–16%) are tabular crystals of oligoclase and hardly of albite ($An_{3–28}$). Biotite (5–8%) occurs as brown or greenish flakes, showing a regular longitudinal cleavage. Phenocrysts enclose zircon and opaque minerals. Sphene (3–5%) is often zoned, and frequently included in feldspars. Ilmenite and magnetite (Mag) are commonly associated with Bt or Spn.

In *Amphibole–Bt-granites*, Qtz is recrystallized and occasionally encloses plagioclase and Kfs. Plagioclase (8–12%) is tabular-shaped albite (Ab) to oligoclase ($An_{1–13}$), often enclosing Bt and opaque minerals. Some plagioclases display bent twin lamellas and deformational kink bands. Kfs ($Or_{92–97}$) are subautomorphic, lath-shaped, and occasionally exhibit perthites. Brown or greenish flakes of Fe-biotite (8–12%) underline foliation and enclose Zrn, Qtz, and amphibole. Fine crystals mould the blasts, or are included in feldspars. Amphibole (8–10%) is hastingsite or Fe-edenite according to [Leake et al. \(1997\)](#). Crystals are brown, green or bluish, pleochroic and often zoned. Spn (< 3%) is interstitial, or locally crystallizes either between Bt–ilmenite contacts or at the edge of ilmenite phenocrystals.

In two *mica–granites*, Qtz (25–35%) is also recrystallized ([Fig. 2e](#)). Phenocrysts commonly enclose Bt and feldspar while microcrystals clog the cracks affecting feldspar phenocrysts. Kfs (25–32%) are orthoclase or microcline ($Ab_{6–92}Or_{5–95}$), sometimes exhibiting distinct cross-hatched and carlsbad twins. Plagioclase (20–25%) is oligoclase and hardly albite ($An_{3–24}$). Phenocrysts are often zoned and exhibit a mechanical cross twinning. Biotite is under the form of brown or greenish flakes composed of Fe-biotite or siderophyllite. Muscovite (4–6%) appears as elongated flakes (XFe: 0.7–1) frequently cleaved. It is commonly included in Kfs, and alters to phengite or Chl. Apatite appears as elongated or hexagonal microcrystals that are either interstitial or in inclusion. Epidote is under the form of brown or green interstitial crystals.

Leucocratic granites crop out in seams of variable thickness (≤ 1 m). Some samples (E_{66}) are pinkish due to their high content of orthoclase. Quartz (36%) forms agglomerates of several crystals associated with feldspars. Kfs (41%) are albite or orthoclase partially altered into Mc. Plagioclases (20%) are tabular crystals of Na-albite and incidentally of oligoclase enclosing fine crystals of Spn.

4. Geochemistry

4.1. Analytical methods

Thirty-two representative samples of plutonics (including mafic intrusions) from Mbengwi have been analyzed by ICP-OES at the “École des mines de Saint-Étienne” (France) for major elements. International geostandards have been used and details of the methods are available in [Benoit et al. \(1996\)](#) and [Aries et al. \(2000\)](#). Isotopic measurements of Sr and Nd on 13 representative samples have been done at Géosciences Environment de Toulouse (GET-OMP–University of Toulouse-3, France). The measurements were eluted after HF/HNO₃ digestion using Eichrom Sr-Spec, Thru-Spec and Ln-Spec resins, and performed on a Finnigan 261 multicollector thermal-ionization mass spectrometer. Sr isotopic ratios are corrected for mass fractionation with normalization to ⁸⁸Sr = 0.1194. Replicate analyses of the NBS 987 standard yielded an average ⁸⁷Sr/⁸⁶Sr value of 0.710255 ± 0.00002 . Nd isotopic data are corrected for mass fractionation by normalization to ratio ¹⁴⁶Nd/¹⁴⁴Nd = 0.7219. Replicate analyses of the La Jolla Nd standard yielded an average ¹⁴³Nd/¹⁴⁴Nd value of 0.511850 ± 0.00001 .

4.2. Major elements characteristics

The Mbengwi plutonics can be subdivided into two not comagmatic and/or not cogenetic major series:

- mafic plutonics displaying SiO₂ contents of 48–52 wt. %;
- intermediate to felsic granitoids (SiO₂: 60.8–77.9 wt. %).

Mafic plutonics plot in the monzodiorite and monzogabbros field (although due to the absence of clinopyroxene, these rocks cannot be considered as monzogabbros but as monzodiorites), while granitoids form a continuous magmatic suite from monzonite to granite in the (Na₂O + K₂O) vs. SiO₂ diagram ([Middlemost, 1994; Fig. 3A](#)).

The normative composition ([Table 1](#)) of granitoids is characterized by (i) the occurrence of acmite in a Bt-granite sample (E_{125}); (ii) and the occurrence of corundum (0.08–2.37 wt. %) in almost all the samples except those containing normative diopside. Mafic plutonics are marked both by the lack of normative Qtz and the occurrence of olivine (2.02–18.9 wt. %) and nepheline (3.48–5.96 wt. %) in almost all the samples. Major elements Harker diagrams display a negative correlation of SiO₂ with Al₂O₃, TiO₂, Fe₂O₃^t, MgO, MnO, and CaO ([Fig. 3B](#)), and a positive correlation of SiO₂ with K₂O both for granitoids and associated mafic intrusions. Decreasing MgO (0.06–8.4 wt. %) and Fe₂O₃^t (0.2–12 wt. %) with increasing SiO₂, Na₂O and CaO reflect the inverse correlation of mafic minerals and feldspar modal contents, even exaggerated by the common replacement of plagioclase with Chl.

All granitoids apart from granodiorites have Na₂O–K₂O < 2 and therefore can be qualified as potassic according to [Le Bas et al. \(1986\)](#). In the K₂O vs. SiO₂ variation diagram ([Fig. 3C](#)) of [Le Maître et al. \(1989\)](#), they

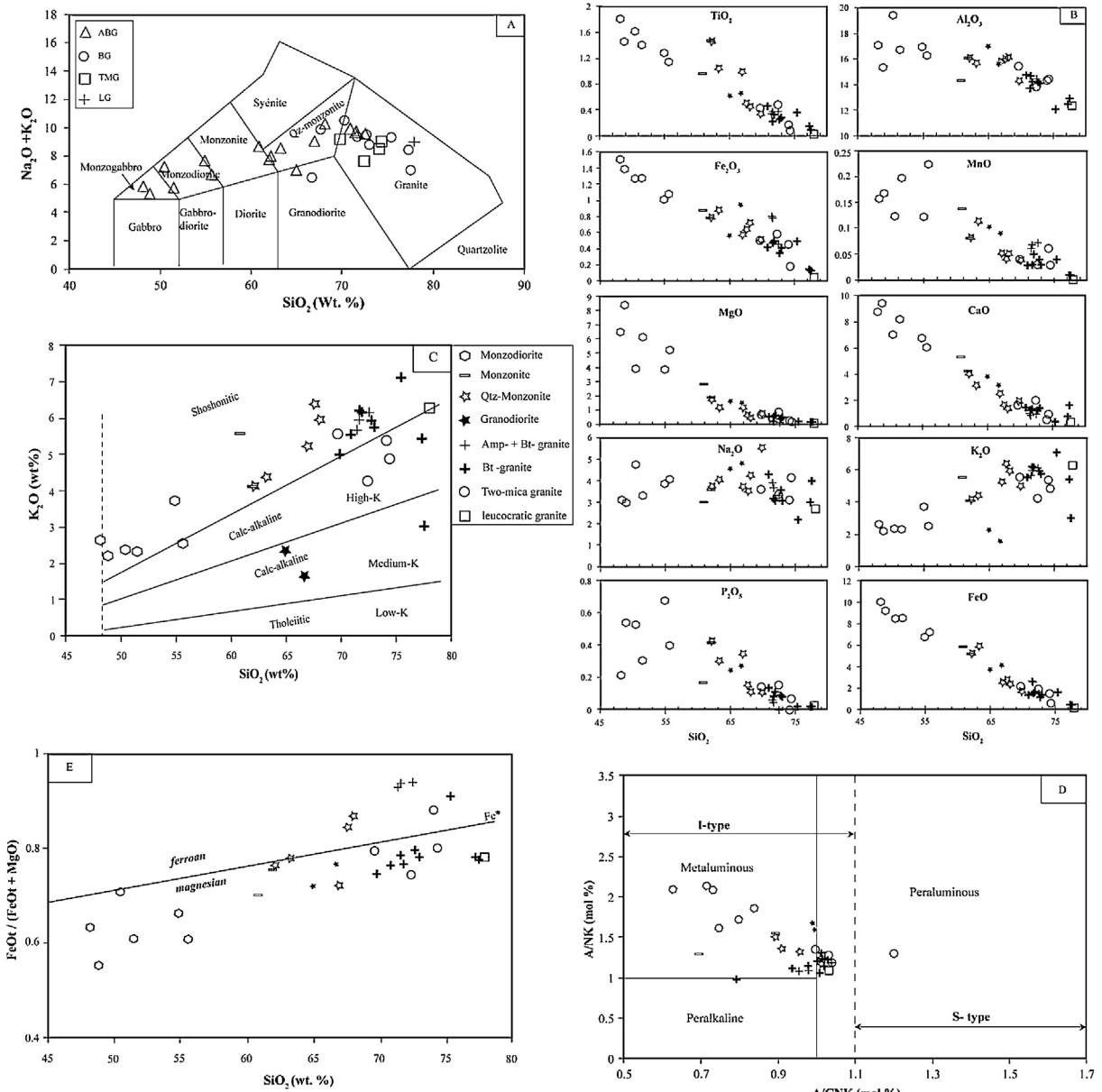


Fig. 3. Chemical classification of the Mbengwi plutonics. A. Composition in the TAS diagram of Middlemost (1994); ABG: amphibole-Bt-granitoids. BG: Bt-granitoids; TMG: two-mica granitoids; LG: leucocratic granite. B. SiO_2 vs. major element (wt. %) diagrams. C. K_2O vs. SiO_2 diagram illustrating the high-K calc-alkaline and shoshonitic affinities of the Mbengwi plutonics. Subdivision after Le Maître et al. (1989) and Rickwood (1989). D. A/NK [$\text{Al}_2\text{O}_3/(\text{Na}_2\text{O} + \text{K}_2\text{O})$] vs. A/CNK [$\text{Al}_2\text{O}_3/(\text{CaO} + \text{Na}_2\text{O} + \text{K}_2\text{O})$] diagram after Maniar and Piccoli (1989). The dashed line represents the boundary between type-I and type-S granites after Chappell and White (1992). E. Plot of $\text{FeO}/(\text{FeO} + \text{MgO})$ vs. SiO_2 with the boundary between ferroan and magnesian fields given by Frost et al. (2001).

plot within the high-K to shoshonitic fields. Only granodiorites and a sample of Bt-granite (E_{20}) occupy the field of the fairly potassic rocks. Their $\text{CaO}/\text{Al}_2\text{O}_3$ molar ratios range from 0.06 to 0.68 and $[(\text{Na}_2\text{O} + \text{K}_2\text{O})/\text{Al}_2\text{O}_3]$ vary from 0.59 to 1.02. According to the diagram of Maniar and Piccoli (1989) and Chappell and White (1992) (Fig. 3D), granitoids are mainly metaluminous to weakly peraluminous in composition. Only a Bt-granite sample containing normative acmite (E_{125}) presents a molar sum $(\text{Na} + \text{K}) > \text{Al}$ and can be considered as peralkaline according to Frost

et al. (2001). The Mbengwi granitoids are mainly of type I, except a two-mica granite (E_{610}) that plots in type-S ($\text{A}/\text{CNK} > 1.1$) field.

Mafic intrusions are potassic ($\text{Na}_2\text{O} - \text{K}_2\text{O} < 2$) according to Le Bas et al. (1986) except monzodiorite (E_{33}). They all plot within the high-K to shoshonitic fields (Fig. 3C), and their $\text{CaO}/\text{Al}_2\text{O}_3$ molar ratios vary from 0.66–1.06, while $[(\text{Na}_2\text{O} + \text{K}_2\text{O})/\text{Al}_2\text{O}_3]$ vary from 0.47 to 0.62. They are metaluminous and of type I ($\text{A}/\text{CNK}: 0.63-0.84$) (Fig. 3D).

Table 1

Whole-rock chemical analyses of representative samples from the Mbengwi plutonics. For the determination of ε_{Nd} and ε_{Sr} we used chondritic uniform reservoir (CHUR) value after De Paolo and Wasserburg (1976) and Uniform reservoir (UR) after Vidal (1994). LG: leucocratic granite; ($^{87}\text{Sr}/^{86}\text{Sr}$)_i: Sr initial ratio.

Samples	Monzodiorite (Mafic intrusions)						Monzonite		Qtz-monzonite			Granodiorite			
	E ₁₄₁	E ₁₃₄	E ₁₃₁	E ₃₃	E ₁₄₂	E ₁₃₅	E _{69b}	E ₆₃	E ₆₇	E ₄₂	E ₁₄₄	E ₆₄	E ₆₅	E ₅₄	E ₄₁
SiO ₂	48.81	48.11	51.44	50.37	55.58	54.84	60.81	61.92	62.11	63.24	66.90	67.57	68.07	64.93	66.64
TiO ₂	1.47	1.82	1.41	1.62	1.15	1.28	0.96	1.48	1.47	1.05	0.99	0.50	0.46	0.64	0.67
Al ₂ O ₃	15.37	17.11	16.74	19.43	16.33	16.96	14.35	16.15	16.10	15.66	15.79	15.98	16.13	17.05	15.69
Fe ₂ O ₃	1.38	1.50	1.28	1.28	1.09	1.02	0.88	0.79	0.79	0.89	0.58	0.64	0.72	0.58	0.96
FeO	9.19	10.00	8.54	8.51	7.24	6.79	5.88	5.26	5.26	5.92	2.57	2.84	2.40	3.85	4.27
MnO	0.17	0.16	0.20	0.12	0.23	0.12	0.14	0.08	0.08	0.11	0.05	0.04	0.05	0.11	0.09
MgO	8.39	6.51	6.19	3.94	5.28	3.91	2.85	1.91	1.79	1.17	1.19	0.64	0.47	1.70	1.59
CaO	9.47	8.81	8.22	7.04	6.07	6.77	5.34	4.25	4.06	3.16	2.57	1.70	1.37	3.93	3.28
Na ₂ O	3.00	3.12	3.32	4.77	4.08	3.88	3.03	3.61	3.74	4.07	3.74	3.53	4.26	4.61	4.88
K ₂ O	2.22	2.65	2.34	2.39	2.55	3.75	5.59	4.12	4.18	4.44	5.28	6.40	5.96	2.35	1.65
P ₂ O ₅	0.53	0.21	0.31	0.53	0.40	0.68	0.17	0.42	0.43	0.30	0.35	0.15	0.11	0.25	0.28
Total (wt.%)	100	100	100	100	100	100	100	100	100	100	100	100	100	100	100
Norm CIPW															
Quartz	-	-	-	-	-	-	6.13	11.89	11.67	11.51	17.39	16.59	15.73	16.25	20.55
Orthose	13.13	15.65	13.84	14.12	15.06	22.17	33.01	24.38	24.70	26.25	31.21	37.80	35.20	13.91	9.77
Albite	18.94	16.13	28.13	29.34	34.53	32.87	25.64	30.51	31.68	34.41	31.69	29.88	36.05	39.02	41.28
Anorthite	21.93	24.86	23.84	24.57	18.72	17.75	9.06	15.71	14.77	11.35	10.46	7.45	6.06	17.84	14.43
Acmite	-	-	-	-	-	-	-	-	-	-	-	-	-	-	-
Nepheline	3.48	5.57	-	5.96	-	-	-	-	-	-	-	-	-	-	-
Diopside	17.60	14.40	12.26	5.75	7.23	9.44	13.60	2.20	2.15	1.99	-	-	-	-	-
Hypersthene	-	-	1.89	-	17.75	5.29	9.06	10.39	10.12	10.51	5.66	5.52	4.32	9.96	10.07
Olivine	18.90	17.27	14.79	14.11	2.02	6.99	-	-	-	-	-	-	-	-	-
Magnetite	2.00	2.17	1.86	1.85	1.57	1.48	1.28	1.14	1.14	1.29	0.84	0.93	1.05	0.84	1.39
Ilmenite	2.79	3.45	2.68	3.08	2.19	2.44	1.82	2.80	2.78	1.99	1.88	0.96	0.87	1.22	1.28
Corindon	0.00	-	-	-	0.00	-	0.00	-	-	-	0.08	0.52	0.45	0.38	0.59
Apatite	1.24	0.49	0.71	1.23	0.93	1.57	0.39	0.97	0.99	0.70	0.80	0.36	0.25	0.58	0.65
TOTAL	100	100	100	100	100	100	100	100	100	100	100	100	100	100	100
DI	35.54	37.36	41.97	49.42	49.59	55.04	64.79	66.78	68.05	72.17	80.28	84.27	86.99	69.18	71.60
Isotopes															
$^{87}\text{Sr}/^{86}\text{Sr}$	0.708199	0.711891	0.707048										0.709809	0.718544	
2σ	0.000009	0.000008	0.000009										0.000009	0.000008	
$^{143}\text{Nd}/^{144}\text{Nd}$	0.512261	0.512405	0.51235										0.512249	0.512229	
2σ	0.000005	0.000006	0.000005										0.000006	0.000007	
Rb	120	154	114										80	91.1	
Sr	862	490	1040										540	262	
Sm	6.87	8.56	9.3										8.67	7.02	
Nd	33.8	36.8	49.1										46.5	30.2	
$^{87}\text{Rb}/^{86}\text{Sr}$	0.389626	0.879935	0.306755										0.414700	0.974164	
$^{147}\text{Sm}/^{144}\text{Nd}$	0.122916	0.140665	0.114545										0.112752	0.140568	
($^{87}\text{Sr}/^{86}\text{Sr}$) _i	0.704576	0.703708	0.704195										0.705952	0.709482	

Table 1 (Continued)

Samples	Monzodiorite (Mafic intrusions)						Monzonite		Qtz-monzonite			Granodiorite					
	E ₁₄₁	E ₁₃₄	E ₁₃₁	E ₃₃	E ₁₄₂	E ₁₃₅	E _{69b}	E ₆₃	E ₆₇	E ₄₂	E ₁₄₄	E ₆₄	E ₆₅	E ₅₄	E ₄₁		
(¹⁴³ Nd/ ¹⁴⁴ Nd)i	0.511118		0.511097	0.511285										0.511202	0.510922		
	Amphibole-biotite granite						Biotite granite						Two-mica granite				
Samples	E ₆₈	E ₆₉	E ₆₁₁	R ₂	E ₂	E ₁₂₅	E ₆	E ₁₂	E ₂₀	E ₅₃	E ₁₂₆	E ₁₂₉	E ₁₄₅	E ₆₁₀	E ₆₀	E ₆₂	
SiO ₂	71.42	71.57	72.46	72.67	71.81	69.80	70.83	75.36	77.51	77.24	72.93	71.60	72.36	74.06	69.65	74.32	77.90
TiO ₂	0.35	0.38	0.38	0.26	0.33	0.34	0.46	0.36	0.09	0.15	0.28	0.23	0.48	0.18	0.43	0.08	0.03
Al ₂ O ₃	13.74	13.77	14.48	14.25	14.24	14.26	14.78	12.13	12.95	12.50	14.08	14.72	13.84	14.36	15.45	14.46	12.36
Fe ₂ O ₃	0.81	0.79	0.46	0.35	0.50	0.51	0.42	0.50	0.13	0.15	0.42	0.48	0.59	0.46	0.50	0.19	0.05
FeO	2.69	2.62	1.54	1.17	1.67	1.71	1.41	1.65	0.45	0.49	1.39	1.60	1.96	1.53	2.24	0.62	0.17
MnO	0.06	0.07	0.07	0.04	0.05	0.04	0.03	0.04	0.01	0.01	0.03	0.03	0.03	0.06	0.04	0.03	0.00
MgO	0.26	0.23	0.13	0.39	0.66	0.75	0.56	0.22	0.16	0.17	0.50	0.56	0.88	0.27	0.69	0.20	0.06
CaO	1.00	0.85	0.97	1.24	1.35	1.95	1.47	0.39	1.63	0.78	1.42	1.29	2.04	0.54	1.65	0.98	0.39
Na ₂ O	3.93	3.70	3.36	3.58	3.10	5.52	4.32	2.21	3.98	3.02	3.09	3.20	3.38	3.13	3.62	4.16	2.71
K ₂ O	5.68	5.97	6.16	5.95	6.18	5.01	5.57	7.12	3.04	5.45	5.78	6.22	4.29	5.41	5.59	4.89	6.30
P ₂ O ₅	0.06	0.05	0.00	0.09	0.11	0.11	0.14	0.02	0.02	0.02	0.08	0.08	0.15	0.00	0.14	0.07	0.02
Total (wt.%)	100	100	100	100	100	100	100	100	100	100	100	100	100	100	100	100	
Norm CIPW																	
Quartz	23.06	23.60	26.20	25.46	25.59	14.59	20.51	33.20	38.74	36.68	28.45	24.84	29.98	32.58	21.67	28.77	37.00
Orthose	33.58	35.30	36.41	35.18	36.49	29.58	32.89	42.10	17.99	32.23	34.15	36.74	25.33	31.95	33.02	28.92	37.26
Albite	33.22	31.33	28.41	30.31	26.21	45.50	36.55	18.68	33.71	25.55	26.15	27.04	28.59	26.48	30.60	35.22	22.97
Anorthite	3.09	3.32	4.81	5.21	5.98	-	4.50	1.80	7.98	3.74	6.51	5.87	9.11	2.68	7.27	4.41	1.82
Acmite	-	-	-	-	-	1.08	-	-	-	-	-	-	-	-	-	-	-
Nepheline	-	-	-	-	-	-	-	-	-	-	-	-	-	-	-	-	-
Diopsidie	1.29	0.50	-	0.29	-	7.50	1.58	-	-	-	-	-	-	-	-	-	-
Hypersthene	3.79	3.98	2.27	2.34	3.84	0.66	2.15	2.64	0.99	0.99	3.06	3.62	4.56	2.93	4.77	1.40	0.36
Olivine	-	-	-	-	-	-	-	-	-	-	-	-	-	-	-	-	-
Magnetite	1.17	1.14	0.67	0.51	0.73	0.20	0.62	0.72	0.20	0.22	0.60	0.69	0.85	0.67	0.73	0.27	0.07
Ilmenite	0.67	0.71	0.71	0.49	0.62	0.64	0.88	0.68	0.17	0.29	0.53	0.43	0.92	0.34	0.82	0.15	0.06
Corindon	-	-	0.53	-	0.27	-	-	0.13	0.18	0.26	0.36	0.58	0.30	2.37	0.79	0.70	0.40
Apatite	0.14	0.11	0.00	0.21	0.26	0.25	0.32	0.05	0.05	0.05	0.19	0.19	0.36	0.00	0.33	0.16	0.05
Total	100	100	100	100	100	100	100	100	100	100	100	100	100	100	100	100	100
DI	89.86	90.23	91.02	90.95	88.30	89.67	89.95	93.98	90.44	94.46	88.75	88.62	83.90	91.01	85.29	92.91	97.23
Isotopes																	
⁸⁷ Sr/ ⁸⁶ Sr	0.746294	0.733343			0.72146		0.738704	0.716319					0.71524	0.787963		0.716392	
2 σ	0.000008	0.000008			0.000008		0.00001	0.000008					0.000007	0.000008		0.000009	
¹⁴³ Nd/ ¹⁴⁴ Nd	0.511793	0.511763			0.512248		0.512559	0.512089					0.511981	0.511594		0.512324	
2 σ	0.000006	0.000007			0.000007		0.000006	0.000008					0.000005	0.000008		0.000007	
Rb	113.5	64.5			178.5		219	86.8					188.5	230		170.5	
Sr	71.2	62.7			272		178.5	217					706	73.3		398	
Sm	18.95	25.4			5		17.8	1.52					5.55	5.43		0.76	
Nd	151.5	232			29.6		65.2	9.5					37.9	24.1		3.6	
⁸⁷ Rb/ ⁸⁶ Sr	4.478438	2.886325			1.839121		3.4442122	1.1204156					0.7477893	8.8516352		1.1999512	
¹⁴⁷ Sm/ ¹⁴⁴ Nd	0.075632	0.066199			0.102149		0.1651055	0.0967521					0.0885489	0.1362298		0.1276662	
(⁸⁷ Sr/ ⁸⁶ Sr)i	0.704645	0.706500			0.704356		0.7066728	0.7058991					0.7082856	0.7056428		0.7052315	
(¹⁴³ Nd/ ¹⁴⁴ Nd)i	0.511090	0.511147			0.511298		0.5110235	0.5111892					0.5111575	0.5103271		0.5111361	

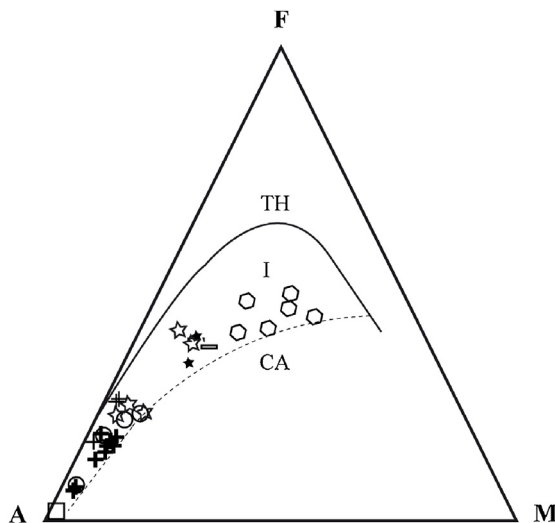


Fig. 4. Plots of the Mbengwi plutonics in the AFM diagram. The boundary between tholeiitic and calc-alkali series (solid line) is after Irvine and Baragar (1971). A = $\text{Na}_2\text{O} + \text{K}_2\text{O}$; F = FeO^t ; M = MgO (wt.%). TH: field of tholeiitic series; I: continental arcs after Brown (1982); CA: field of calc-alkali series.

The I-type geochemical signature of the studied plutonics is supported by the mineralogy (predominance of Hbl, Bt as mafic silicate minerals, and the abundance of Spn and Mag as accessory phases). The $\text{FeO}^t/(\text{MgO} + \text{FeO}^t)$ ratios of mafic plutonics (0.56–0.71) are lower than those of granitoids ranging between 0.70–0.94, but both series predominantly plot in the magnesian field (Fig. 3E).

4.3. Sr–Nd isotopic results

In order to characterize the sources of the Mbengwi plutonics, we carried out Rb/Sr and Sm/Nd isotopic analyses on three monzodiorites and ten granitoids (two granodiorites, two amphibole-Bt- granites, three Bt- granites, two two-mica granites, and one leucocratic granite). The Nd, Sm, Sr, Rb contents and various isotopic ratios of the analyzed samples are presented in Table 1. Isotopic data have been corrected from an age of 620 My,

according to the fact that no precise geochronological ages exist for our samples. All the analyzed samples have measured ${}^{87}\text{Sr}/{}^{86}\text{Sr}$ ratios higher than 0.7050 (average isotopic composition of the continental crust). However, one of the two-mica granite (E₆₁₀) has a very high ${}^{87}\text{Sr}/{}^{86}\text{Sr}$ value (0.78796). The initial ${}^{87}\text{Sr}/{}^{86}\text{Sr}$ isotopic ratios of mafic intrusions vary from 0.70371 to 0.70458, whereas the initial ε_{Nd} values range between -1.8 (E₁₄₁) and +0.6 (E₃₃). These same parameters vary respectively from 0.70436 to 0.70948 and from -15.9 to +0.7 in granitoids. The most enriched granitoids, in terms of ε_{Nd} , is a Bt-granite (E₁₂) and the most depleted sample is a two-mica granite (E₆₁₀). ${}^{87}\text{Rb}/{}^{86}\text{Sr}$ ratios vary from 0.31 to 0.88 in mafic intrusions, and from 0.42 to 8.85 in granitoids. The Sm/Nd ratios are rather constant, either in the analyzed mafic intrusions (0.11–0.14) or in the analyzed granitoids (0.07–0.16). Therefore, age corrections are critical for the Rb/Sr system and have a lesser impact on the Sm/Nd radioactive couple.

5. Discussion and conclusion

5.1. Magmatic affinity and nature of the magma source

Using both the TAS diagram of Middlemost (1994; Fig. 3A) and AFM diagram (Fig. 4), it is noticeable that the Mbengwi plutonic suite occupies the fields of calc-alkaline series. In the AFM diagram, the representative points all integrate area I, forming a crescent shape characteristic of calc-alkaline series. This calc-alkaline affinity is also evidenced by a positive correlation of their Fe^* ($\text{FeO}^t/[\text{FeO}^t + \text{MgO}]$) (Frost et al., 2001) with SiO_2 contents (Fig. 3E). All the mafic intrusions have magnesian affinity. Despite the presence of some Qtz-monzonite and granites having ferric affinity ($0.85 \leq \text{Fe}^* < 0.95$), almost all the granitoids samples are also magnesian. These same characteristics have been identified for Ngondo (Tagne-Kamga, 2003), Nkambe (Tetsopgang et al., 2008) and the western Cameroon granitoids in general (Nzolang, 2005).

Trace element and Sr isotope data can be used to more robustly decipher the nature of a magma source. Chemically mafic intrusions are metaluminous, have a low total alkali content (5.2–7.6) low FeO^t/MgO (1.2–2.5) and low

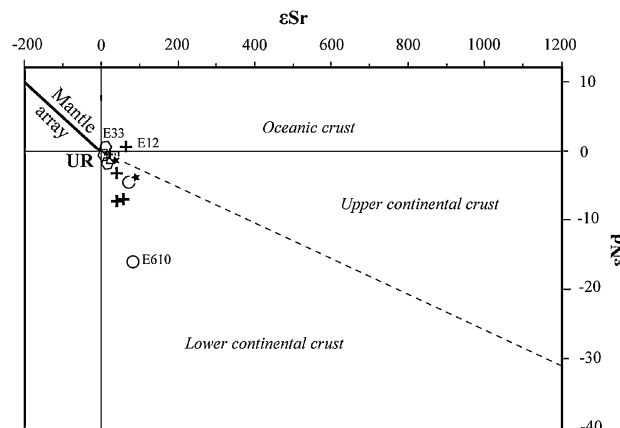


Fig. 5. Location of the Mbengwi plutonics sources using the diagram of Foucarde (1998).

Mg# values (29–44.3). Granitoids are weakly peraluminous, have a high total alkali content (mostly > 8.1 wt. %), low FeO^T/MgO (with very few > 5) and lower Mg# values (< 30). The overall low Mg# of the studied rocks rule out:

- the possible direct melting of a peridotitic mantle source that was metasomatized via the addition of slab melt;
- or the interaction of slab partial melts with peridotite during ascent through the mantle wedge (Martin et al., 2005);
- or else magma mixing between crust- and mantle-derived melts (Jiang et al., 2009).

In addition, their high-K calc-alkaline geochemical characteristics are not consistent with an origin via an interaction between slab partial melts and peridotite during ascent through the mantle wedge. Experiments of partial melting in conditions of temperatures and pressures close to reality (Patino Douce and Beard, 1996; Singh and Johanneses, 1996) proved that granitoids magmas can be produced from a wide range of parental crustal rocks. The REE patterns of Mbengwi granitoids and associated mafic intrusions exhibit LREE enrichment ($[\text{La}/\text{Yb}]_N > 10$), are mainly high in total REE (> 200 ppm), and have negative Eu anomalies. These REE characteristics are inconsistent with those of mantle-derived rocks, suggesting that these magmas originated in the crust. All the analyzed samples have $\varepsilon_{\text{Sr}} > 0$, which is symptomatic of a crustal source. Therefore, the investigated rocks may result from partial melting of the continental crust and the linearity of binary plots for the Mbengwi suite either for granitoids or for mafic intrusions can be explained mostly as a result of fractional crystallization. The monzodiorite sample (E_{33}) seems to be the less differentiated rock of the mafic series considering its lowest $^{87}\text{Sr}/^{86}\text{Sr}$ ratio, although it does not have a radiogenic ε_{Nd} . The type-S two-mica granite (E_{610}) with its high SiO₂ content (74.04 wt. %) is among the most evolved rock of the analyzed intermediate and felsic series; its lowest ε_{Nd} value (-15.86) is evocative of its long and complex crustal history.

The coupling of Sr and Nd tracers in the diagram of Foucarde (1998; Fig. 5) enables to accurately locate the source of these Pan-African rocks. Almost all result from the melting of the lower continental crust, except the less differentiated mafic intrusion (E_{33}) and a sample of Bt-granite (E_{12}) having positive ε_{Nd} , symptomatic of the oceanic crust source. The ε_{Nd} vs. SiO₂ wt. % variation diagram (not shown) reveals a general lack of correlation between these two parameters for all the studied rocks. This suggests that the variability of isotopic contents is the consequence of the heterogeneity of sources. However, the positive and negative correlations observed respectively for the mafic intrusions and for intermediate to felsic granitoids (granodiorites, amphibole-Bt-granites and two-mica granites) may be furthermore an argument in favor of the involvement of AFC processes. In granites, the values of ε_{Sr} , ε_{Nd} , and of the $^{87}\text{Sr}/^{86}\text{Sr}$ and $^{87}\text{Rb}/^{86}\text{Rb}$ isotopic ratios vary significantly, contrary to their SiO₂ contents (71.5–75.4 wt. %). These characteristics also observed in the syn-orogenic granitoids from the Bandombaaï complex in

Namibia are likely related to the assimilation of intermediate rocks (probably granodiorite or tonalite) from the lower crust, which would have greatly modified the isotopic composition (Van de Flierdt et al., 2003).

5.2. Tectonic context

The geodynamic context of the Mbengwi plutonics has been inferred using their amounts of major elements, Rb, Y and Nb. Major elements geochemistry of Mbengwi granitoids and associated mafic intrusions points to the high-K shoshonitic and calc-alkaline affinity of the investigated samples, implying a subduction- to collision-related geotectonic setting.

In the (Y + Nb) vs. Rb diagram of Pearce (1996), the studied rocks are mostly post-collisional, except two granites samples (E_{66} , E_{129}) that integrate the field of syn-collision. All the mafic intrusions plot in the field of volcanic arc granites (VAG), except E_{142} , which occupies the field of within plate granites (WPG). The granitoids clearly occupy as other western Cameroon Pan-African granitoids, such as those of Bantoum (Nzolang et al., 2003), Bafoussam (Djouka-Fonkwé et al., 2008), Nkambe (Tetsopgang et al., 2008) and even those of the NE-Brazil (Guimarães et al., 2004) both the areas of VAG and that of WPG (Fig. 6a). In the (Nb/Zr)_N vs. Zr variation diagram of Thiéblemont and Tegyey (1994; Fig. 6b), almost all mafic intrusions plot in the post-COLG domain and only two occupy the field of the subduction zone. Monzonites, Qtz-monzonites, granodiorites, amphibole-Bt-granites, and most of two-mica granites occupy the field of post-collisional rocks; while the majority of Bt-granites rather integrate the field of rocks associated with subduction zones. In general, we notice that samples are spread from the area of rocks associated with subduction zones (VAG) to that of post-collisional granitoids. These characteristics and mostly the high-K calc-alkaline to shoshonitic affinity of the Mbengwi granitoids and the associated mafic intrusions are commonly reported in granitoids from late-collision to post-collision continental settings (Black and Liégeois, 1993; Liégeois et al., 1994, 1998; Toteu et al., 2004). The evolution from high-K cal-alkaline to shoshonitic or alkaline-peralkaline compositions observed in the studied granitoids is typical of final stages of orogeny (post-collision) in a continental collisional setting where crustal delamination operated (Liégeois et al., 1994, 1998). The overall geochemical features are similar to those of western and central Cameroon Pan-African granitoids related to the Pan-African D₁ event in Cameroon (Kwékam et al., 2010; Nguissi Tchankam et al., 1997; Nzolang et al., 2003) and to those of the Ngondo complex (Tagne-Kamga, 2003), but differ from common granitoids from the magmatic arc (e.g., Pearce et al., 1984; Pimentel et al., 1996) by their distinctive depletion in Sr- and Y-undepleted pattern (not shown). The Mbengwi plutonics are slightly different from the Ngaoundéré granitoids (Tchameni et al., 2006) by the absence of samples including the area of within plate alkaline rocks. Therefore, some within-plate features observed in some granitoids (Fig. 6a) may be interpreted as an evolved trend of calc-alkaline suites (Tchameni et al., 2006). The geochemical subduction-type signature shown

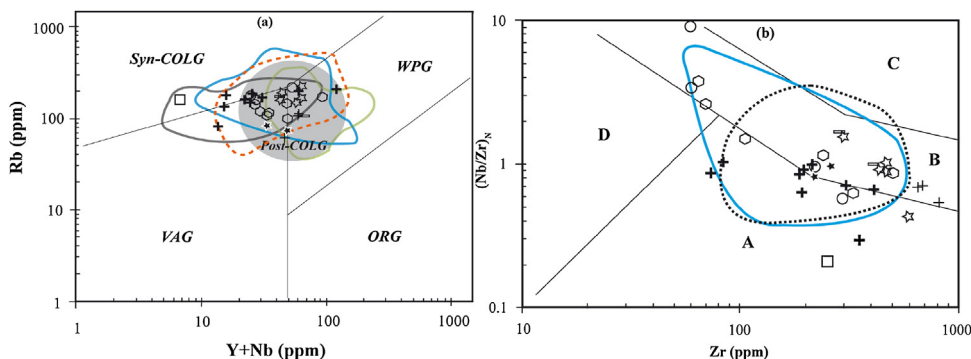


Fig. 6. Tectonic discrimination of the Mbengwi plutonics. (a) Rb vs. (Y + Nb) diagram with discriminative fields after Pearce (1996): the red dash line represents the field of Pan-African granitoids of NE-Brazil (Guimarães et al., 2004), the black line represents the domain of Nkambe granitoids (Tetsopang et al., 2008), green line is that of Bantoum granitoids (Nzolang, 2005) and blue line is that of granitoids from Bafoussam (Djouka-Fonkwe et al., 2008). (b) Plots of the Mbengwi plutonics in Zr vs. (Nb/Zr)_N diagram, with discriminative fields after Thiéblemont and Tegvey (1994): the blue line represents the domain of granitoids from Bafoussam (Djouka-Fonkwe et al., 2008), dashed line is that of granitoids from Ngaoundéré (Tchameni et al., 2006). Normalization to chondrite values from McDonough and Sun (1995).

by the studied rocks would probably be inherited from their protolithes, emplaced during the subduction phase preceding the collision.

The ongoing study, including mineralogy, trace element geochemistry, and further U/Pb dating on zircon, will enable us to characterize more tightly the petrogenesis and melting processes of the Mbengwi granitoids and the associated mafic rocks.

Acknowledgements

The authors are grateful to the French Ministry of Foreign Affairs for providing a grant to B.J. Mbassa for his 12-month stay in France, EGIDE and GET-UMR 5563-CNRS for analytical facilities and logistics. Profs. Georges Ceuleneer and Jacek Puziewicz are thanked for their constructive comments and suggestions that greatly led to a considerable improvement of the manuscript.

References

- Aries, S., Valladon, M., Polvé, M., Dupré, B.A., 2000. Routine method for oxide and hydroxide interference corrections in ICP-MS chemical analyses of environmental and geological samples. *Geostand. News.* 24, 19–31.
- Benoit, M., Polvé, M., Ceuleneer, G., 1996. Trace element and isotopic characterization of mafic cumulates in a fossil mantle diapir (Oman ophiolite). *Chem. Geol.* 134, 199–214.
- Black, R., Liégeois, J.-P., 1993. Cratons, mobile belts, alkaline rocks and continental lithospheric mantle: the Pan-African testimony. *J. Geol. Soc. London* 150, 89–98.
- Brown, G.C., 1982. Calc-alkaline intrusive rocks: their diversity, evolution and evolution to volcanic arcs. In: Thorpe, R.S. (Ed.), *Andesites*. Wiley, New York, pp. 437–460.
- Chappell, B.W., White, A.J.R., 1992. I-and S-type granites in the Lachlan Fold Belt. *Trans. Royal Soc. Edinburgh: Earth Sci.* 83, 1–26.
- De Paolo, D.I., Wasserburg, G.J., 1976. Nd isotopic variations and petrogenetic models. *Geophys. Res. Lett.* 3, 249–253.
- Djouka-Fonkwe, M.L., Schulz, B., Schüssler, U., Tchouankoué, J.-P., Nzolang, C., 2008. Geochemistry of the Bafoussam Pan-African I-and S-type granitoids in western Cameroon. *J. Afr. Earth Sci.* 50, 148–167.
- Foucarde, S., 1998. Les isotopes : effets isotopiques, bases de radio-géochimie. In: Hagemann, G., Treuil, M. (Eds.), *Introduction à la géochimie et ses applications*. CEA, Paris, pp. 265–495.
- Frost, B.R., Arculus, R.J., Barnes, C.G., Collins, W.J., Ellis, D.J., Frost, C.D., 2001. A geochemical classification of granitic rocks. *J. Petrol.* 42, 2033–2048.
- Guimarães, I.P., Da Silva Filho, F.A., Almeida, C.N., Van Schmus, W.R., Araújo, M.M.J., Melo, S.C., Melo, E.B., 2004. Brasiliano (Pan-African) granitic magmatism in the Pajeú–Paraíba belt, Northeast Brazil: an isotopic and geochronological approach. *Precambrian Res.* 135, 23–53.
- Irvine, T.N., Baragar, W.R.A., 1971. A guide to the chemical classification of the common volcanic rocks. *Can. J. Earth Sci.* 8, 523–548.
- Jiang, Y.H., Jiang, S.Y., Dai, B.Z., Liao, S.Y., Zhao, K.D., Ling, H.F., 2009. Middle to Late Jurassic felsic and mafic magmatism in southern Hunan province, southeast China: implications for a continental arc to rifting. *Lithos* 107, 185–204.
- Kretz, R., 1983. Symbols of rock-forming minerals. *Am. Mineral.* 68, 277–279.
- Kwékam, M., Liégeois, J.-P., Njonfang, E., Affaton, P., Hartmann, G., Tchoua, M.F., 2010. Nature, origin and significance of the Fomopéa Pan-African high-K calc-alkaline plutonic complex in the Central African fold belt (Cameroon). *J. Afr. Earth Sci.* 57, 79–95.
- Leake, B.E., et al., 1997. Nomenclature of amphiboles: report of the subcommittee on amphiboles of the International Mineralogical Association, commission on new minerals and mineral names. *Am. Mineral.* 82, 1019–1037.
- Le Bas, M.J., Le Maître, R.W., Streckeisen, A., Zanetti, B., 1986. A chemical classification of volcanic rocks based on the total alkali-silica diagram. *J. Petrol.* 27, 745–750.
- Le Maître, R.W., Bateman, P., Dubek, A., Keller, J., Lameyre, J., Le Bas, M.J., Sabine, P.A., Schmid, R., Sorensen, H., Streckeisen, A., Woolley, A.R., Zanetti, B., 1989. A classification of igneous rocks and glossary of terms. Recommendations Int. Union Geol. Sci. Sub commission on the Systematic of Igneous rocks. Oxford, Blackwell, 193 p.
- Liégeois, J.-P., Black, R., Navez, J., Latouche, L., 1994. Early and Late pan-African orogenies in the Aïr assembly of terranes (Tuareg Shield, Niger). *Precambrian Res.* 67, 59–88.
- Liégeois, J.-P., Navez, J., Hertogen, J., Black, R., 1998. Contrasting origin of post-collisional high-K calc-alkaline and shoshonitic versus alkaline and peralkaline granitoids. The use of sliding normalization. *Lithos* 45, 1–28.
- Maniar, P.D., Piccoli, P.M., 1989. Tectonic discrimination of granitoids. *Geol. Soc. Am. Bull.* 101, 635–643.
- Martin, H., Smithies, R.H., Rapp, R., Moyen, J.F., Champion, D., 2005. An overview of adakite, tonalite-trondhjemite-granodiorite (TTG), and sanukitoid: relationships and some implications for crustal evolution. *Lithos* 79 (1–2), 1–24.
- Mbassa B.J., 2015. Petrographic, mineralogical, geochemical and geochronological characterizations of the magmatic formations from Mbengwi (NW-Cameroon, central Africa). Ph.D thesis, Univ. Yaoundé I, 231p.
- Mbassa, B.J., Njonfang, E., Benoit, M., Grégoire, M., Kamgang, P., Duchene, S., Brunet, P., Ateba, B., Tchoua, M.F., 2012. Mineralogy, geochemistry and petrogenesis of the recent magmatic formations from Mbengwi, a continental sector of the Cameroon Volcanic Line (CVL), Central Africa. *Mineral. Petrol.* 106, 217–242.
- McDonough, W.F., Sun, S.-S., 1995. The composition of the Earth. *Chem. Geol.* 120, 223–253.

- Middlemost, E.A.K., 1994. Naming material in the magma/igneous rock system. *Earth Sci. Rev.* 37, 215–224.
- Nédélec, A., Macaudière, J., Nzenti, J.-P., Barbey, P., 1986. Évolution structurale et métamorphique des schistes de Mbalmayo (Cameroun). Implication sur la structure de la zone mobile panafricaine d'Afrique Centrale au contact du craton du Congo. *C. R. Acad. Sci. Paris Ser. II* 303, 75–80.
- Ngako, V., Affaton, P., Njonfang, E., 2008. Pan–African tectonics in north-western Cameroon: implication for the history of western Gondwana. *Gondwana Res.* 14, 509–522.
- Ngnotué, T., Nzenti, J.-P., Barbey, P., Tchoua, F.M., 2000. The Ntui–Bétamba high-grade gneisses: a northward extension of the panafrican–Yaoundé gneisses in Cameroon. *J. Afr. Earth Sci.* 31, 369–381.
- Nguissi Tchankam, C., Nzenti, J.-P., Nsifa, E.N., Tempier, P., Tchoua, M.F., 1997. Les granitoïdes calco-alcalins, syn-cisaillement de Bandja dans la chaîne panafricaine nord-équatoriale au Cameroun. *C. R. Acad. Sci. Paris, Ser. IIa* 325, 95–101.
- Njanko, T., Nédélec, A., Affaton, P., 2006. Synkinematic high-K calc-alkaline plutons associated with the Pan–African Central Cameroon shear zone (W-Tibati area): Petrology and geodynamic significance. *J. Afr. Earth Sci.* 44, 494–510.
- Nzenti, J.-P., Barbey, P., Macaudière, J., Soba, D., 1988. Origin and evolution of the Late Precambrian high grade Yaoundé gneisses (Cameroon). *Precambrian Res.* 38, 91–109.
- Nzolang, C., 2005. Crustal evolution of the Precambrian basement in west Cameroon: inference from geochemistry, Sr–Nd isotopes and experimental investigation of some granitoids and metamorphic rocks. Ph.D. thesis, Niigata Univ. Japan, 207 p.
- Nzolang, C., Kagami, H., Nzenti, J.-P., Holtz, F., 2003. Geochemistry and preliminary Sr–Nd isotopic data on the Neoproterozoic granitoids from the Bantoum area, West Cameroon. Evidence for a derivation from a Paleoproterozoic to Archean crust. *Polar Geosci.* 16, 196–226.
- Patino Douce, A.E., Beard, J.S., 1996. Effects of P, f(O₂) and Mg/Fe ratio on dehydration melting of model metagreywackes. *J. Petrol.* 37, 999–1024.
- Pearce, J.A., 1996. Sources and setting of granitic rocks. *Episodes* 19 (4), 120–125.
- Pearce, J.A., Harris, N.B.W., Tindle, A.G., 1984. Trace elements discrimination diagrams for the geotectonic interpretation of granite rocks. *J. Petrol.* 25, 956–983.
- Penaye, J., Toteu, S.F., Michard, A., Bertrand, J.M., Dautel, D., 1989. Reliques granulitiques d'âge Protérozoïque inférieur dans la zone mobile panafricaine d'Afrique centrale au Cameroun : géochronologie U/Pb sur zircons. *C. R. Acad. Sci. Paris, Ser. II* 309, 315–318.
- Pimentel, M.M., Fuck, A.R., Souza de Alvarenga, C.J., 1996. Post-Brasiliano (Pan-African) high-K granitic magmatism in central Brazil: the role of Late Precambrian-Early Paleozoic extension. *Precambrian Res.* 80, 217–238.
- Rickwood, P.C., 1989. Boundary lines within petrologic diagrams which use oxides of major and minor elements. *Lithos* 22, 247–264.
- Singh, J., Johannessen, W., 1996. Dehydration melting of tonalites: Part II. Composition of melts and solids. *Contrib. Mineral. Petrol.* 125, 26–44.
- Tagne-Kamga, G., 2003. Petrogenesis of the Neoproterozoic Ngondo Plutonic complex (Cameroon, west central Africa): a case of late collisional ferro-potassic magmatism. *J. Afr. Earth Sci.* 36, 149–171.
- Tchameni, R., Pouclet, A., Penaye, J., Ganwa, A.A., Toteu, S.F., 2006. Petrography and geochemistry of the Ngaoundéré Pan–African granitoids in central North Cameroon: Implications for their sources and geological setting. *J. Afr. Earth Sci.* 44, 543–560.
- Tetsopang, S., Suzuki, K., Njonfang, E., 2008. Petrology and CHIME geochronology of Pan–African high-K and Sr/Y granitoids in the Nkambe area, Cameroon. *Gondwana Res.* 14, 686–699.
- Thiéblemont, D., Tegyey, M., 1994. Une discrimination géochimique des roches différenciées témoin de la diversité d'origine et de situation tectonique des magmas calco-alcalins. *C. R. Acad. Sci. Paris, Ser. II* 319, 87–94.
- Toteu, S.F., Van Schmus, R.W., Penaye, J., Michard, A., 2001. New U–Pb and Sm–Nd data from north-central Cameroon and its bearing on the pre-Pan–African history of central Africa. *Precambrian Res.* 108, 45–73.
- Toteu, S.F., Penaye, J., Poudjom Djomani, Y., 2004. Geodynamic evolution of the Pan–African belt in central Africa with special reference to Cameroon. *Can. J. Earth Sci.* 41, 73–85.
- Van de Flieerd, T., Hoernes, S., Jung, S., Masberg, P., Hoffer, E., Schaltegger, U., Friedrichsen, H., 2003. Lower crustal melting and the role of open-system processes in the genesis of syn-orogenic quartz diorite–granite–leucogranite associations: constraints from Sr–Nd–O isotopes from the Bandombaa Complex, Namibia. *Lithos* 67, 205–226.
- Vidal, P., 1994. Géochimie. Dunod, Paris, 190 p.